Carbon-*K*-shell molecular-frame photoelectron angular distributions in the photoisomerization of neutral ethylene

N. Douguet,[1] T. N. Rescigno,[2] and A. E. Orel[1]

[1]*Department of Chemical Engineering and Materials Science, University of California, Davis, California 95616, USA*

[2]*Lawrence Berkeley National Laboratory, Chemical Sciences and Ultrafast X-ray Science Laboratory, Berkeley, California 94720, USA*

(Received 10 June 2013; published 15 July 2013)

Photoexcitation of neutral ethylene to its V state can initiate conformational changes of the molecule. The migration of one hydrogen atom to another carbon site occurs via a nonadiabatic passage and leads to the formation of a stable and asymmetric ethylidene isomer. We present the carbon-K-shell molecular-frame photoelectron angular distributions (MFPADs) calculated at relevant geometries in the isomerization of ethylene. The theoretical results are compared with available experimental data at the ground-state geometry of ethylene. Despite the complexity of this system and the presence of two heavy atomic centers, the main features of the photoisomerization of ethylene can be traced through the shape of the MFPADs.

DOI: 10.1103/PhysRevA.88.013412 PACS number(s): 33.80.Eh

I. INTRODUCTION

Photoisomerization is a light-initiated chemical process in which a polyatomic molecule undergoes conformational changes from one isomeric form to another. Various types of geometry changes can occur, from simple bond twisting or atom migration, to more complicated processes, such as ring opening polymerization. Therefore, photoisomerization converts photon energy to mechanical motion and can trigger important biochemical processes in vision (e.g., opening and closing of the iris), in division of melanocytes (tanning), or in photosynthesis. A new generation of light sources, such as the free electron laser [1], coupled with improvements in high-order-harmonic generation techniques [2,3], offers the possibility of probing an isomerization reaction by quasi-instantaneous imaging the internal structure of a molecule. Molecular-frame photoelectron angular distributions (MFPADs) have been proposed as a method of obtaining information about such photoisomerization reactions, since the electron-wave (photoelectron), launched through photoabsorption, is diffracted by the potential of a molecule in a way that its angular distribution in the fixed-body frame can be used as a probe of the molecular geometry.

In order to recover the photoionization characteristics in the fixed-body frame, suitable experimental techniques have to be used. The observation of the MFPADs requires fixed orientation of the molecule, which can, for instance, be achieved through three-dimensional laser alignment [4–6] by inhibiting the free rotation of the target in all three Euler angles. However, this is not a suitable experimental technique in photoisomerization reactions for which the conformation of the molecule changes very rapidly over time (∼10–100 fs). Another experimental method [7] consists of using cold target recoil ion momentum spectroscopy (COLTRIMS) in which the molecular orientation for event is recorded by measuring in coincidence core-hole photoelectron and ion fragments following prompt Auger decay (Coulomb explosion). The latter idea was successfully applied in K-shell photoionization of ground-state methane [8], for which a three-dimensional picture of the four C-H bonds was obtained and excellent agreement between the theoretical calculations and the experimental measurements was achieved. In the latter study, it was found that the photoelectron angular distribution, when averaged over the direction of light polarization, shows that the scattering occurs predominantly along the chemical bonds of the target molecule. The same feature was also theoretically predicted for ammonia and water [9]. The average over polarization directions is particularly easy to record in a COLTRIMS experiment, where the molecular target is of course randomly oriented in the laboratory frame, and such averaging actually improves the statistics.

The imaging of molecular bonds via MFPADs is a striking result, which has yet only been observed for molecules with a unique heavy center. Molecules involved in photoisomerization possess several heavy centers and the K-shell MFPADs may not image such molecules. In our previous study [10] of K-shell photoisomerization of the acetylene monocation $C_2H_2^+$ we found strong variations in the form of MFPADs with respect to geometry changes along the isomerization path, making it possible to differentiate the linear, trans, and vinylidene conformations of $C_2H_2^+$. However, beyond exhibiting the correct symmetry of the fixed-nuclei target, it was noticed that the MFPADs do not simply image the molecule, but possess a more complicated structure. We speculated that multiple scattering effects from the two carbon atoms might be responsible for the complicated additional structure we observed.

There are significant experimental difficulties and limitations in performing COLTRIMS experiments on $C_2H_2^+$ photoisomerization, which requires a valence photoionization step to produce the target monocation and a second x-ray photon to probe the conformational change. Here we study neutral ethylene photoisomerization, which is directly initiated by photoexcitation to its V state. In the following section, we will briefly describe the main characteristics of ethylene photoisomerization (electronic state, reaction path, and photoionization). In Sec. III, we describe our theoretical model based on the complex Kohn variational method and discuss the salient features of our *ab initio* calculations. A comparison between our results and available COLTRIMS experimental data for carbon K-shell MFPADs on ethylene ground state is given in Sec. IV A. Calculated MFPADs at

the main geometries in ethylene photoisomerization, namely, for planar geometry (initial state), twisted ethylene (transition state), twisted-pyramidalized ethylene (conical intersection), and ethylidene (isomer) is given in Sec. IV B. Finally, Sec. V is devoted to our conclusions.

II. DESCRIPTION OF ETHYLENE PHOTOISOMERIZATION

First-principles photodynamics of ethylene has been extensively studied by Ben-Nun and Martinez [11], with emphasis on the complicated shape of the V state potential electronic surface (PES) and the critical role of conical intersections. It is now widely accepted that conical intersections, i.e., true crossings of multidimensional potential surfaces, exist at energies accessible to photoexcited molecules and play a crucial role in many photochemical processes [12–15]. The experimentally measured lifetime of excited ethylene is 30 ± 15 fs [16], which suggests that the molecule decays from the valence state back to the ground state through a conical intersection. Indeed, Ben-Nun and Martinez have found no less than eight conical intersections involving the V state that are likely to play a role in the photochemistry of ethylene, which points to the high complexity of the dynamics. Nevertheless, it was found by Ben-Nun and Martinez [11] that quenching to the ground electronic state of ethylene proceeds primarily through conical intersections characterized by twisting and pyramidalization, which confirmed a previous finding of Freund and Klessinger [17]. Recently, an XUV pump-probe experiment was performed on ultrafast internal conversion in ethylene photoisomerization [18]. They studied the mechanisms and pathways for quenching by measuring the CH_2^+ and CH_3^+ fragmentation channels as a function of time delay. By using an *ab initio* multiple spawning method, which confirmed the observed CH_2^+/CH_3^+ relative peak height, it was concluded that 72% of the nonradiative events occur through a twisted-pyramidalized conical intersection and 28% through an ethylidene-like conical intersection.

Even for a relatively small molecule like C_2H_4, the dynamics of the isomerization can be a rather complicated process. The important conformations for the ethylene photoisomerization are depicted in Fig. 1. Photoexcitation of ethylene to its V state promotes an electron from a bonding π molecular orbital into an antibonding π^* molecular orbital, thus reducing the C-C bond order. The planar geometry of ethylene is not a stable conformation on the V state, so elongation and twisting of the C-C bond occurs, leading to a lower energy conformation in D_{2d} symmetry (90° twisting). It was once believed that the latter twisted conformation represents a global minimum on the V state PES; however, it was found in Refs. [11] and [17] that it is not a true minimum, but is rather a saddle point. From this transition state, the migration of a hydrogen atom can occur, either directly through the C-C bond on the V state towards the ethylidene-like conical intersection (such a path has, for instance, been found in [11]), which is geometrically close to the final ethylidene minimum, or more likely by pyramidalization towards the twisted or pyramidalized conical intersection and back to the N state via a nonadiabatic passage.

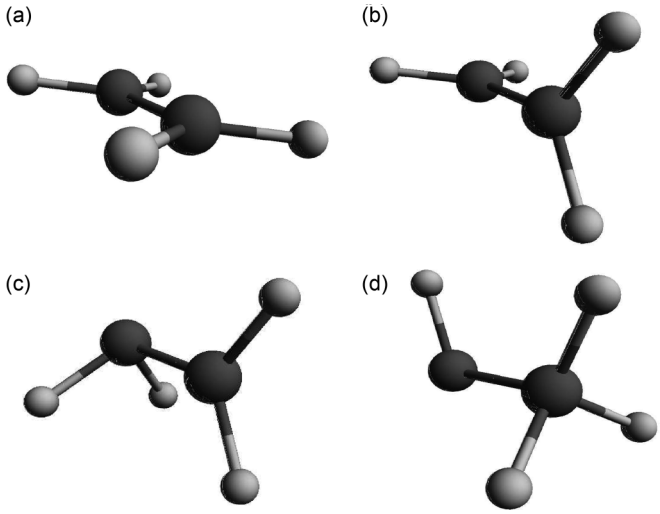

FIG. 1. Principal geometries considered in ethylene photoisomerization: (a) planar geometry (initial state), (b) twisted (transition state), (c) twisted-pyramidalized (conical intersection), and (d) ethylidene (isomer).

In the present study, we do not intend to further describe the dynamics of ethylene photoisomerization, but instead focus on K-shell photoelectron angular distributions at the important geometries introduced above. In all results presented below, we have used internal structures of ethylene reported by Ben-Nun and Martinez [11].

III. THEORETICAL APPROACH

The photoionization cross section is determined from the following matrix element expressed in terms of body-frame amplitudes:

$$I^{\mu}_{\Gamma_o l_o m_o} \equiv \langle \Psi_o | \mu \left| \Psi^{-}_{\Gamma_o l_o m_o} \right\rangle = \sum_{i=1}^{N} \int \Psi_o(r_1, r_N) r_i^{\mu} \Psi^{-}_{\Gamma_o l_o m_o}(r_1, r_N) d^3 r_1 \cdots d^3 r_N, \tag{1}$$

where the function Ψ_o represents the initial state of the target molecule, $\Psi^{-}_{\Gamma_o l_o m_o}$ is the wave function describing the final ionized state, and r^{μ} is the dipole operator defined in the length form as

$$r^{\mu} = \begin{cases} z, \mu = 0 \\ \mp (x \pm iy)/\sqrt{2}, \mu = \pm 1. \end{cases} \tag{2}$$

In the present study, the wave function describing the final ionized state is determined using the complex Kohn variational method. The complex Kohn method has been descibed in detail previously [19,20]. The implementation of the Kohn principle in calculations of photoionization cross sections and photoelectron angular distributions has also been presented previously [9,10,21,22], thus we only recap the main ideas in the following development.

In the Kohn method, the wave function representing the electron-ion scattering, with the ion in a state Γ_o, is expressed

as

$$\Psi^{-}_{\Gamma_o l_o m_o} = \sum_{\Gamma} \hat{A}\left(\chi_\Gamma F^{-}_{\Gamma\Gamma_o}\right) + \sum_i d_i^{\Gamma_o}\Theta_i, \tag{3}$$

where the first sum runs over the energetically open ionic states described by $(N-1)$-electron wave functions χ_Γ and the second sum runs over N-electron configuration-state functions Θ_i. The operator $\hat{A}$ ensures the antisymmetrization between the continuum and bond ionic wave functions. The continuum functions $F^{-}_{\Gamma\Gamma_o}$ are expanded as

$$F^{-}_{\Gamma\Gamma_o} = \sum_i c_i^{\Gamma\Gamma_o}\phi_i(r) + \sum_{lm}\left[f_l(k_\Gamma r)\delta_{ll_o}\delta_{mm_o}\delta_{\Gamma\Gamma_o} + T^{\Gamma\Gamma_o}_{ll_o mm_o} h_l^{-}(k_\Gamma r)\right]Y_{lm}(\hat{r})/r, \tag{4}$$

where f_l and h_l^{-} are partial-wave continuum radial functions behaving asymptotically as regular and incoming Coulomb functions and ϕ_i is a set of square integrable functions. Applying the Kohn variational principle to Eq. (1) gives a set of linear equations for the coefficients $c_i^{\Gamma\Gamma_o}$, $d_i^{\Gamma_o}$, and $T^{\Gamma\Gamma_o}_{ll_o mm_o}$.

To obtain an amplitude representing an ejected electron with momentum $\boldsymbol{k}_{\Gamma_o}$ associated with a particular ion channel and direction of light polarization $\hat{\epsilon}$, the matrix element in Eq. (1) must be combined in a partial wave series

$$I_{\hat{k}_{\Gamma_o},\hat{\epsilon}} = \sqrt{\frac{4\pi}{3}} \sum_{l_o m_o \mu} i^{l_o} e^{-i\delta_{l_o}} I^{\mu}_{\Gamma_o} Y^{*}_{1\mu}(\hat{\epsilon}) Y^{*}_{l_o m_o}\left(\hat{k}_{\Gamma_o}\right), \tag{5}$$

and the doubly differential cross section for a hypothetical space-fixed target molecule is thus given as

$$\frac{d^2\sigma^{\Gamma_o}}{d\Omega_{\hat{k}}\, d\Omega_{\hat{\epsilon}}} = \frac{8\pi\omega}{3c}\left|I_{\hat{k}_{\Gamma_o},\hat{\epsilon}}\right|^2, \tag{6}$$

where c is the speed of light and ω is the photon energy. Using Eqs. (5) and (6) and the orthonormality of the spherical harmonics $Y^{*}_{1\mu}(\hat{\epsilon})$, the following expression for the body-frame differential cross section, averaged over all polarization directions, is readily derived:

$$\int \frac{d^2\sigma^{\Gamma_o}}{d\Omega_{\hat{k}}\, d\Omega_{\hat{\epsilon}}} d\Omega_{\hat{\epsilon}} = \frac{32\pi^2\omega}{9c} \sum_{\mu} \left| \sum_{l_o m_o} I^{\mu}_{\Gamma_o l_o m_o} Y_{l_o m_o}\left(\hat{k}_{\Gamma_o}\right) \right|^2. \tag{7}$$

The calculations are performed using a set of optimized molecular orbitals and a reference space in which both core-hole ionic states χ_Γ and the initial neutral state Ψ_o are described through a complete active space (CAS) calculation. In order to obtain a suitable set of molecular orbitals, as well as a reference space of manageable size, we used natural orbitals averaged over the two core-hole states. This choice gave a good description of these states and an accurate K-shell ionization energy. In contrast, using orbitals optimized for the neutral state overestimates the ionization energy by more than 10 eV.

In all results presented below, we used the correlation-consistent, polarized valence triple-zeta (cc-pvtz) basis of Dunning [23], a reference space of ten molecular orbitals, keeping three electrons in the two carbon K-shell orbitals, and a virtual space [i.e., the functions denoted as ϕ_i in Eq. (4)] of 104 functions. This choice allows us to include in the active space the full set of carbon $2p$ orbitals, so that all spatial directions are treated on an equal footing. The molecular geometries in the ethylidene configuration, as well as near the conical intersection, have no symmetry (C_1 point group). Therefore, to ensure consistency among the different geometries, we did not use symmetry in any of the calculations. These prescriptions resulted in ionic core-hole wave function with ∼1400 terms and an initial target wave of ∼330 terms. Combing these with the basis of 104 virtual space orbitals resulted in variational trial functions with ∼150 000 terms.

Finally, we have also checked convergence in the shape of the MFPADs with respect to the size of the reference space, by performing calculations with a reference space of nine and also 11 orbitals (freezing the $2s$ orbitals for the latter calculation) and observed negligible variations in the photoelectron angular distribution. On the other hand, low-energy results at the static-exchange level were not satisfactory, meaning that scattering by ethylene monocation is sensitive to the inclusion of electron correlation and target-distortion effects.

IV. RESULTS

A. Recoil-frame K-shell photoelectron angular distributions

Osipov *et al.* [24] have recently carried out an experimental COLTRIMS study of carbon K-shell photoionization of

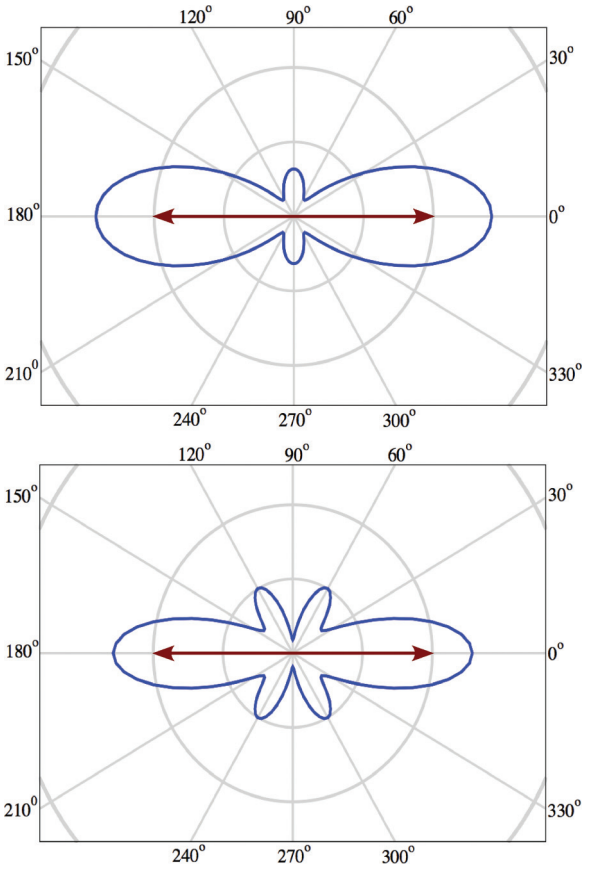

FIG. 2. (Color online) Electron angular distribution at 293 eV photon energy for light polarization direction (red arrow) along the molecular axis: A_u core hole (upper panel) and A_g core hole ×2 (lower panel).

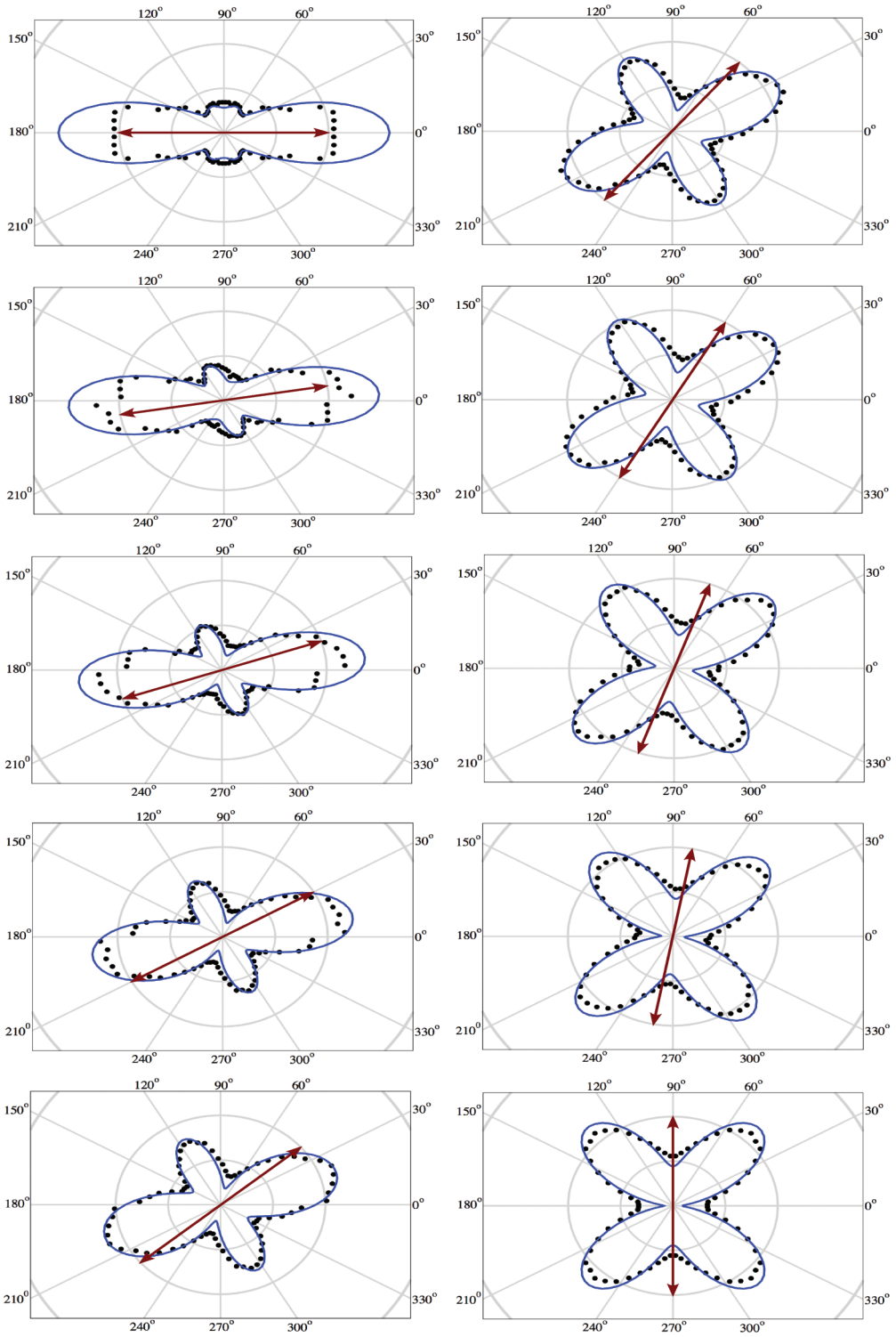

FIG. 3. (Color online) Electron angular distribution, at 293 eV photon energy, as a function of light polarization direction (red arrow) from 0° to 90°. The molecular axis is always along the x axis. The theoretical results (blue solid line) have been averaged over an opening angle of ±10° and compared with experimental values (black dots) of Ref. [24].

ground-state C_2H_4. Comparison with these results provides an opportunity to test the accuracy of our theoretical calculations. In this experiment, only the C-C recoil axis was determined, not the relative orientation of the CH_2^+ fragments. Therefore, to allow for a meaningful comparison, we averaged our calculated MFPADs over the unobserved azimuthal angle.

Osipov *et al.* measured the recoil-frame K-shell photoelectron angular distributions (RFPAD) at several photon energies as a function of the direction of light polarization with respect

to the recoil axis. The experimental results were compared with a simple spherical harmonic fitting formula as well as the results of theoretical calculations using the Kohn-Sham B-spline linear combination of atomic orbitals formalism [25,26]. The theoretical calculations reproduce particularly well the experimental measurement at photoelectron energies above 10 eV, but discrepancies arise at lower energy, when polarization effects and electron correlations play an important role.

Our calculated K-shell ionization energy from ethylene ground state is 287.9 eV, in very good agreement with the experimental measurement [24] of 288 eV. Osipov *et al.* performed one set of measurements just above the K-shell ionization threshold, at 293 eV photon energy. We investigated electron angular distributions at the corresponding photoelectron energy of 5 eV, for both ungerade (A_u) and gerade (A_g) core holes, at the planar equilibrium ground-state geometry of ethylene (D_{2h}). The results are presented in Fig. 2, for light polarization direction (arrow) along the molecular axis. It is important to note that, for clarity, the A_g cross section in Fig. 2 was rescaled by a factor 2 with respect to the A_u cross section. In addition to the predominant electron emission along the molecular axis, additional structure is present at 60°, 120°, 240°, and 300° for the A_g core hole, in a Y_3^0-like pattern, and at directions perpendicular to the molecular axis for the A_u core hole, in a Y_2^0-like pattern. Note that the symmetry of the dominant spherical harmonic in the photoelectron angular distribution is consistent with the associated symmetry of the molecular hole for a σ cross section ($\hat{\epsilon}$ parallel to the molecular axis). The calculated difference in ionization energy to form either a A_u or a A_g core hole was ∼60 meV, which was not resolved in the experiment. Therefore, to allow direct comparison with experiment, we summed the cross sections for both core-hole final states.

In Fig. 3, we have plotted our summed RFPADs versus the experimental data for light polarization directions from 0° to 90° with respect to the molecular axis. Our theoretical data was averaged over the experimental finite acceptance angle of $\Delta\theta = \pm 10°$. The theoretical calculations agree very well with the experimental data, faithfully reproducing the shape of the angular distributions. We should note that for photoelectron energies above 10 eV (not shown), our results agree with both experiment and previous theory.

B. MFPADs for ethylene photoisomerization

Our three-dimensional MFPADs for the K-shell photoionization of ground-state ethylene at its equilibrium geometry, averaged over all polarization directions [8], are shown in Fig. 4. We plot separately the MFPADs to both core-hole final states, as well as their sum. In this figure, and all figures below, all MFPADs are shown in arbitrary units. As can be seen in the figure, electron emission along the C-H and C=C bonds dominate so that the MFPADs roughly image the conformation of ethylene.

Figure 5 shows MFPADs at the same geometry, but now for K-shell photoionization from the excited V state which can be reached by photoabsorption of photons of ∼8 eV and above. There are only minor differences between the results shown in Figs. 4 and 5, confirming our earlier findings [10] that, at the same photoelectron energy, the K-shell MFPADs are sensitive to nuclear geometry but not to the valence electronic configuration of the photoionized species.

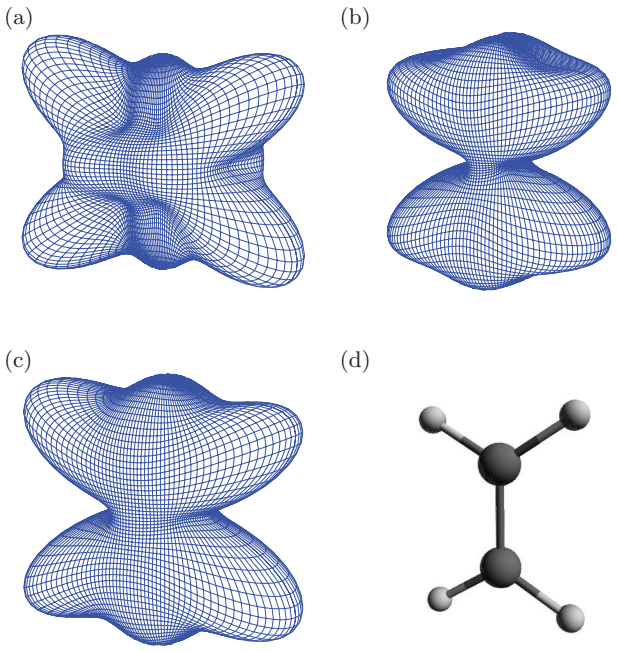

FIG. 4. (Color online) Three-dimensional K-shell MFPADs for ethylene planar equilibrium geometry from the N state: (a) A_g core hole, (b) A_u core hole, (c) averaged $A_g + A_u$ core hole, and (d) geometry representation. The photoelectron energy is 5 eV.

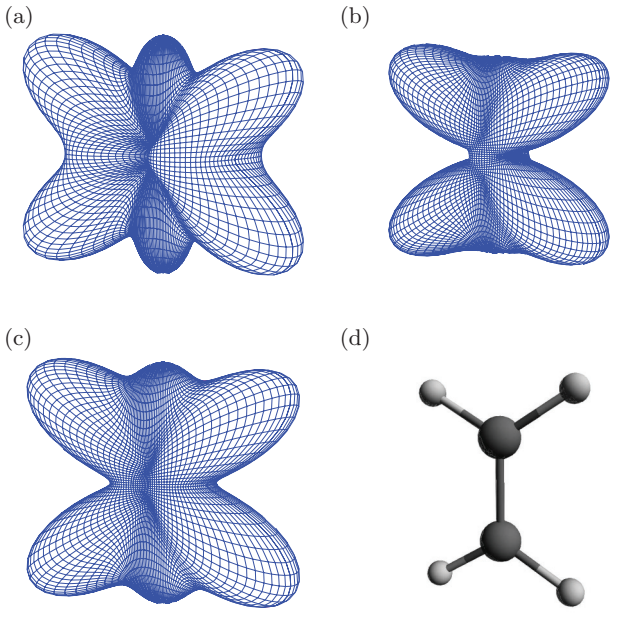

FIG. 5. (Color online) Three-dimensional K-shell MFPADs for ethylene planar geometry (same as in Fig. 4) following pumping to the excited V state: (a) A_g core hole, (b) A_u core hole, (c) averaged $A_g + A_u$ core hole, and (d) geometry representation. The photoelectron energy is 5 eV.

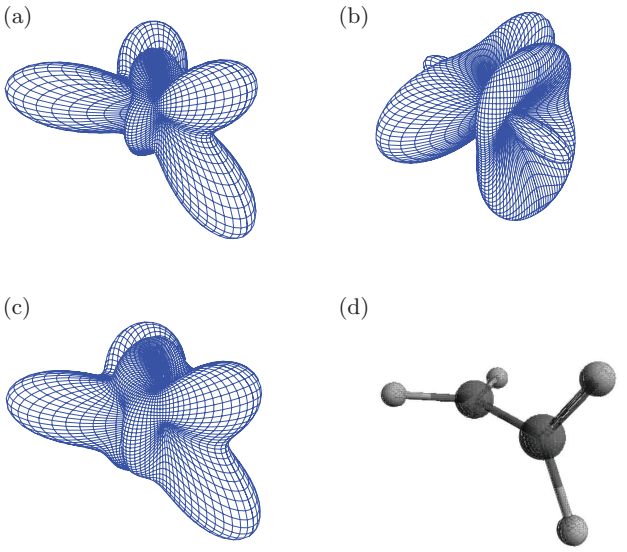

FIG. 6. (Color online) Three-dimensional K-shell MFPADs for ethylene twisted geometry (transition state) from the excited V state: (a) B_2 core hole, (b) A_1 core hole, (c) averaged $B_2 + A_1$ core hole, and (d) geometry representation. The photoelectron energy is 5 eV.

The twisted geometry of ethylene is an important conformation in the photoisomerization process. Once an electron is promoted from the π to the antibonding π^* molecular orbital, twisting and elongation of the C-C bond occurs, until the two CH_2 planes become orthogonal to each other and the molecule reaches a transition state (saddle point) in D_{2d} symmetry. Corresponding MFPADs from the excited V state are presented in Fig. 6, for an electron removed from a K-shell molecular orbital, with either A_1 or B_2 (antisymmetric with respect to rotation reflection) irreducible representation. At 5 eV photoelectron energy, the largest differential photoionization cross section is again to the antisymmetric core-hole molecular orbital. The maximum emission is about 28 Kb/sr to form the B_2 core hole and only 12 Kb/sr to form the A_1 core hole. Both core-hole MFPADs exhibit the rotation-reflection symmetry, however, only the B_2 core-hole MFPAD seems to image the C-H bonds. Note that, as in the case of ethylene ground state, we have observed that at higher photoelectron energy, the cross section to the symmetric core-hole state starts to dominate and is characterized by a large enhancement in emission along the C-C axis. This feature is actually quite general and occurs at all studied geometries. To track conformational changes, therefore, experiments should be carried out close to threshold. At the twisted geometry, the core-hole splitting is still small. Therefore, we also show the polarization-averaged MFPADs, summed over both core-hole states, in the same figure. Again, we find a propensity for photoelectron emission along the C-C and C-H bonds.

Departing from the transition state, hydrogen migration can occur, either directly on the V state PES until the ethylidene conical intersection is reached, or through a pyramidalization bending towards the twisted or pyramidalized conical intersection (Sec. II). We calculated the MFPADs near this twisted or pyramidalized conical intersection. The latter calculations had to be undertaken with care due to the proximity in energy of the electronic states close to the conical intersection. In generating

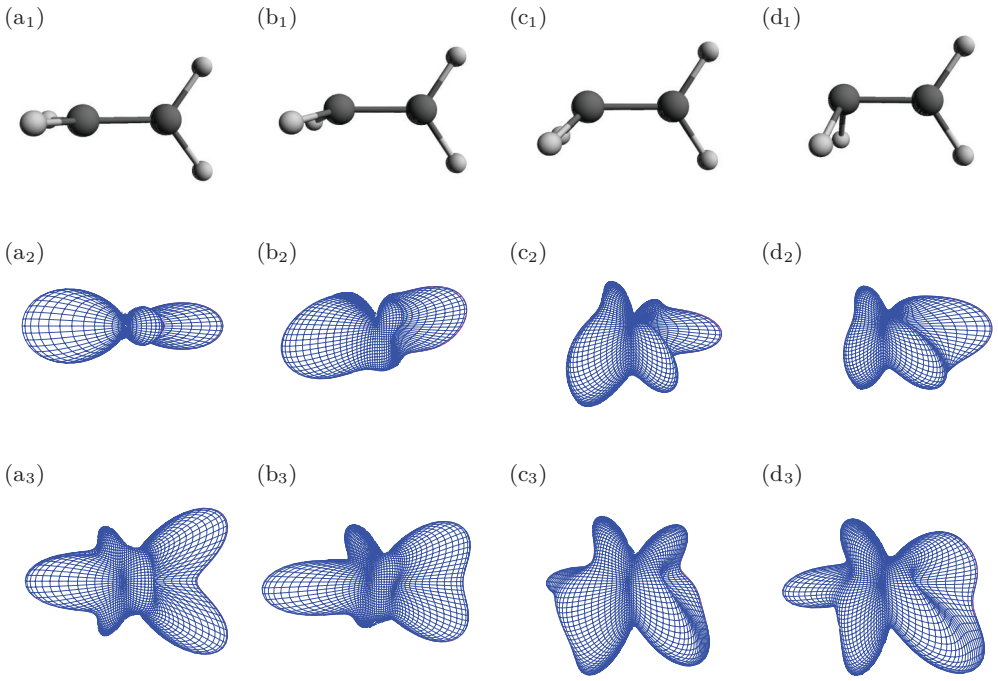

FIG. 7. (Color online) Transverse view of the change in the MFPADs as a function of the pyramidalization angle, from the transition state geometry towards the conical intersection: (a) 0°, (b) 20°, (c) 45°, and (d) 80° pyramidalization angles. The upper line depicts the geometry of the molecule, the middle line represents the MFPADs for K-shell photoionization from the core hole in the carbon atom involved in the pyramidalization (localized hole on the carbon atom on the left side of the figure), and the bottom line represents the MFPADs averaged over both core-hole photoionizations. The photoelectron energy is 5 eV at all geometries.

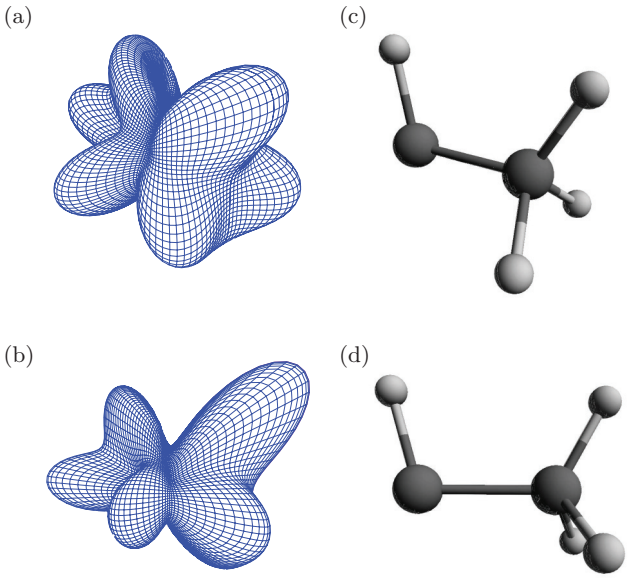

FIG. 8. (Color online) Three-dimensional K-shell MFPADs for ethylidene geometry (isomer) from the N state: (a) and (b) represent two different views of the MFPAD at ethylidene geometry and (c) and (d) are the corresponding geometry representations. The photoelectron energy is 5 eV.

optimized molecular orbitals, it was important to maintain consistency in choosing which core-hole states to average. The results are presented in Fig. 7, where we plot MFPADs at different geometries, from the twisted conformation (0° angle of pyramidalization) to the conical intersection (80° angle of pyramidalization). Note that the intermediate path between these two conformations has not been determined from a steepest descent calculation, but rather by applying manually a smooth variation of the geometries. On the top line of the figure, a transverse view of the geometries of ethylene is shown, at 0°, 20°, 45°, and 80° twisted or pyramidalized bending angles.

As soon as the D_{2d} symmetry is broken, the carbon sites are no longer equivalent and core-hole localization occurs. In fact, we have calculated that the energy gap between the core-hole states increases to a few tenths of an eV, such that it might be feasible to resolve site-specific photoelectrons. The MFPADs corresponding to the core hole on the carbon site involved in the twisted or pyramidalization of ethylene are plotted on the second line of Fig. 7. There is a relative diminution of the emission along the C-H bonds as the geometry gets closer to the conical intersection and some additional structures are observed. On the bottom line of the figure, the MFPADs summed over the two core holes are presented.

Finally, once the migration of a hydrogen atom from one carbon site to the other has occurred, it results in the formation of the ethylidene isomer, representing a local minimum on the N-state PES. This conformation, which completes the photoisomerization of ethylene, has a geometrical structure with a high level of asymmetry, which leads to an equivalent complexity in its MFPAD. As discussed previously, when a large asymmetry in the chemical structure exists between the two carbon sites, the energy gap between the two core-hole states is correspondingly large and can be experimentally resolved with sub-eV detection. Interestingly, the sum of the MFPADs over the two core-hole states gives a comprehensible picture of the ethylidene geometry and the corresponding results are plotted in Fig. 8 at two different views of the molecule to facilitate the three-dimensional visualization. The summed MFPAD still depicts its main emissions along the chemical bonds, despite the overall complexity in the positioning of the hydrogen atoms with respect to the C-C axis. Enhanced emission along the C-C and C-H bonds is clearly observed, along with the addition of smaller secondary lobes.

V. CONCLUSION

Using the complex Kohn variational method, we have investigated carbon K-shell molecular-frame photoelectron angular distributions along the dominant photoisomerization path of ethylene. Our results were compared to available COLTRIMS experimental data on core-level recoil-frame photoelectron angular distributions from ground-state ethylene and good agreement was observed. Our theoretical study confirms the promising idea that changes in the conformation of ethylene along its isomerization path can be tracked through carbon K-shell molecular-frame photoelectron angular distributions. Furthermore, we have shown that the twisted or pyramidalization of ethylene close to a conical intersection can be traced by this technique and could contribute to an understanding of this complicated chemical process. Hopefully, a time-resolved UV-pump–x-ray probe experiment, coupled with COLTRIMS detection, will fulfill the promise of getting snapshots of a chemical reaction in real time in the not-too-distant future.

ACKNOWLEDGMENTS

This work was performed under the auspices of the US DOE by LBNL under Contract No. DE-AC02-05CH11231 and was supported by the US DOE Office of Basic Energy Sciences, Division of Chemical Sciences. A.E.O. acknowledges support by the National Science Foundation, with some of the material based on work done while serving at NSF. The authors wish to thank R. Lucchese for helpful discussions and contributions in improving the computational efficiency of the codes used in this study.

[1] W. Ackermann *et al.*, Nat. Photonics **1**, 336 (2007).
[2] G. Sansone *et al.*, Science **314**, 443 (2006).
[3] E. Gouliemakis *et al.*, Science **320**, 1614 (2008).
[4] P. Hockett, C. Z. Bisgaard, O. J. Clarkin, and A. Stolow, Nat. Phys. **7**, 612 (2011).
[5] J. L. Hansen *et al.*, Phys. Rev. A **83**, 023406 (2011).

[6] J. J. Larsen, K. Hald, N. Bjerre, H. Stapelfeldt, and T. Seideman, Phys. Rev. Lett. **85**, 2470 (2000).
[7] R. Dorner *et al.*, Phys. Rep. **330**, 95 (2000).
[8] J. B. Williams *et al.*, Phys. Rev. Lett. **108**, 233002 (2012).
[9] C. S. Trevisan, C. W. McCurdy, and T. N. Rescigno, J. Phys. B: At. Mol. Opt. Phys. **45**, 194002 (2012).
[10] T. N. Rescigno, N. Douguet, and A. E. Orel, J. Phys. B: At. Mol. Opt. Phys. **45**, 194001 (2012).
[11] M. Ben-Nun and T. J. Martinez, Chem. Phys. **259**, 237 (2000).
[12] M. Klessinger and J. Michl, *Excited States and Photochemistry of Organic Molecules* (VCH Publishers, New York, 1995).
[13] D. R. Yarkony, J. Chem. Phys. **104**, 7866 (1996).
[14] W. Domcke and G. Stock, Adv. Chem. Phys. **100**, 1 (1997).
[15] Mohamed El-Amine Madjet, O. Vendrell, and R. Santra, Phys. Rev. Lett. **107**, 263002 (2011).
[16] P. Farmanara, V. Stert, and W. Radloff, Chem. Phys. Lett. **288**, 518 (1998).
[17] L. Freund and M. Klessinger, Int. J. Quantum Chem. **70**, 1023 (1998).
[18] T. K. Allison *et al.*, J. Chem. Phys. **136**, 124317 (2012).
[19] T. N. Rescigno, B. H. Lengsfield, and C. W. McCurdy, *Modern Electronic Structure Theory* (World Scientific, Singapore, 1995), Vol. 1, p. 501.
[20] T. N. Rescigno, C. W. McCurdy, A. E. Orel, and B. H. Lengsfield, III, *Computational Method for Electron-Molecule Collisions* (Plenum Press, New York, 1995), p. 1.
[21] T. N. Rescigno, B. H. Lengsfield, and A. E. Orel, J. Chem. Phys. **99**, 5097 (1993).
[22] N. Douguet, T. N. Rescigno, and A. E. Orel, Phys. Rev. A **86**, 013425 (2012).
[23] T. H. Dunning, Jr., J. Chem. Phys. **90**, 1007 (1989).
[24] T. Osipov, M. Stener, A. Belkacem, M. Schoffler, T. Weber, L. Schmidt, A. Landers, M. H. Prior, R. Dorner, and C. L. Cocke, Phys. Rev. A **81**, 033429 (2010).
[25] D. Toffoli, M. Stener, G. Fronzoni, and P. Decleva, Chem. Phys. **276**, 25 (2002).
[26] M. Stener, Chem. Phys. Lett. **356**, 153 (2002).